

Vortex Phase Qubit: Generating Arbitrary, Counterrotating, Coherent Superpositions in Bose-Einstein Condensates via Optical Angular Momentum Beams

Kishore T. Kapale^{1,*} and Jonathan P. Dowling^{2,3}

¹*Quantum Computing Technologies Group, Jet Propulsion Laboratory, California Institute of Technology, Mail Stop 126-347, 4800 Oak Grove Drive, Pasadena, California 91109-8099, USA*

²*Hearne Institute for Theoretical Physics, Department of Physics & Astronomy, Louisiana State University, Baton Rouge, Louisiana 70803-4001, USA*

³*Institute for Quantum Studies, Department of Physics, Texas A&M University, College Station, Texas 77843, USA*

(Received 4 May 2005; published 19 October 2005)

We propose a scheme for the generation of arbitrary coherent superpositions of vortex states in Bose-Einstein condensates (BEC) using the orbital-angular-momentum states of light. We devise a scheme to generate coherent superpositions of two such counterrotating states of light using well-known experimental techniques. We show that a specially designed Raman scheme allows for transfer of the optical vortex-superposition state onto an initially nonrotating BEC. This creates an arbitrary and coherent superposition of a vortex and antivortex pair in the BEC. The ideas presented here could be extended to generate entangled vortex states, design memories for the orbital-angular-momentum states of light, and perform other quantum information tasks. Applications to inertial sensing are also discussed.

DOI: [10.1103/PhysRevLett.95.173601](https://doi.org/10.1103/PhysRevLett.95.173601)

PACS numbers: 42.50.Ct, 03.67.-a, 03.75.Gg, 03.75.Lm

Generation and manipulation of macroscopic superpositions, as well as entangled states, is of paramount interest to the field of quantum information [1]. In this regard, Bose-Einstein condensates (BEC) [2] come across as ideal candidates. BECs correspond to highly coherent macroscopic ground states of the confining potentials. Moreover, vortex states of BECs, which are topological states with special phase structure, have been realized experimentally [3]. Stirring a BEC cloud with laser beams leads to the nucleation of vortex lattices in the BEC. These vortex states are fairly stable and could be candidates for qubits in quantum information processors, if appropriate means to manipulate them are developed.

In an entirely different area of optical physics, tremendous progress has been made in creation [4–6], manipulation [7], detection [8,9], and application [10] of the orbital-angular-momentum (OAM) states of light. The OAM states have a corkscrew-type helical phase structure. To illustrate, an OAM state with angular momentum $\hbar\ell$ has $|\ell|$ azimuthal phase singularities across a cut taken in the beam path. The sign of ℓ corresponds to the sense of rotation of the phase fronts around the beam axis. Each photon in the OAM beam carries an orbital-angular momentum of $\hbar\ell$. The quantum nature of these OAM states has been demonstrated recently by showing that a photon pair created in parametric down-conversion process is entangled in the orbital-angular-momentum space along with the usual polarization entanglement [11].

Excitation of vortices in BECs, using the optical vortex beams, has been proposed recently using Raman techniques [12,13] and using slow light techniques [14]. In this Letter we introduce a scheme for creation of macroscopic superpositions of BEC vortex states through transfer of angular momentum of light from specially prepared

OAM-state superpositions. These should be compared to recent macroscopic superpositions of counterrotating electrons in the superconducting flux qubits [15].

Generation of the superposition of Gaussian beams with OAM states of light has been demonstrated [16]. Our interest, however, lies in creating an arbitrary superposition of two counterrotating optical vortices.

The OAM states of light have unique amplitude and phase structures. To illustrate, monochromatic OAM beams have an azimuthal phase dependence of the type $\exp(i\ell\phi)$. Laguerre-Gaussian (LG) laser modes are an example of such OAM states [17]. The normalized LG mode at the beam waist ($z = 0$) and beam size w_0 at the waist is given in cylindrical coordinates (ρ, ϕ, z) by

$$\text{LG}_p^\ell(\rho, \phi) = \sqrt{\frac{2p!}{\pi(|\ell| + p)!}} \frac{1}{w_0} \left(\frac{\sqrt{2}\rho}{w_0}\right)^{|\ell|} L_p^{|\ell|} \left(\frac{2\rho^2}{w_0^2}\right) \times \exp(-\rho^2/w_0^2) \exp(i\ell\phi), \quad (1)$$

where $L_p^\ell(\rho)$ are the associated Laguerre polynomials,

$$L_p^{|\ell|}(\rho) = \sum_{m=0}^p (-1)^m \frac{(|\ell| + p)!}{(p - m)! (|\ell| + m)! m!} \rho^m; \quad (2)$$

w_0 is the beam width, p is the number of nonaxial radial nodes of the mode, and the index ℓ , referred to as the winding number, which describes the helical structure of the wave front around a phase dislocation. For further discussion we consider only pure LG modes with charge ℓ and $p = 0$; we denote such a state of the light field by $|\ell\rangle$ such that $\langle \mathbf{r} | \ell \rangle = \text{LG}_0^\ell(\rho, \phi)$. Thus the states $|+\ell\rangle$ and $|-\ell\rangle$, with ℓ being a whole number, differ only in the sense of the winding of the phase—either clockwise or counterclockwise. Our aim is to create a general superpo-

sition of the OAM states of light of the kind: $(a_+|\ell\rangle + a_-|-\ell\rangle)$, with $|a_+|^2 + |a_-|^2 = 1$. It is well known that creation of superposition of OAM states of the kind $\sum_\ell c_\ell|\ell\rangle$ is a fairly straightforward procedure by using computer generated holographs [5] or phase plates [6]. Moreover, a sorter of these OAM states has also been demonstrated [9] that can distinguish and separate different OAM components. Thus, by using a mixed OAM-state generator and a OAM sorter in conjunction one can easily obtain a pure OAM state $|\ell\rangle$.

We note that dove prisms can be used to change the handedness of light beams passing through them [18]. Consequently, the sense of the phase winding of an LG beam would be reversed as it passes through a dove prism. Using this, we devise a Mach-Zender type configuration as shown in Fig. 1 to generate a general superposition $(\tilde{r}|\ell\rangle + \tilde{r}'|-\ell\rangle)$ at one of the output ports of the interferometer. The first beam splitter is taken to be a special beam splitter with the ratio of $i\tilde{r}:\tilde{r}'$ for the transmitted and the reflected amplitudes at its output ports. The second beam splitter is a usual 50:50 beam splitter.

The operation of the Mach-Zender configuration of Fig. 1 can be described through the matrix representation of beam-splitter operation [19], such that the initial state $(|\ell\rangle, 0)^T$ transforms into

$$\frac{1}{\sqrt{2}} \begin{pmatrix} \tilde{r}|\ell\rangle + \tilde{r}'|-\ell\rangle \\ i(\tilde{r}|\ell\rangle - \tilde{r}'|-\ell\rangle) \end{pmatrix} \quad (3)$$

at the exit ports 1 and 2 of the Mach-Zender Interferometer, respectively, with the choice of $\phi = \pi$. Thus, by ignoring port 2 and renormalizing the state from port 1 we obtain the required superposition state $\tilde{r}|\ell\rangle + \tilde{r}'|-\ell\rangle$, as $|\tilde{r}|^2 + |\tilde{r}'|^2 = 1$. In the following we present our scheme for transferring this optical vortex state superposition to BEC vortex superpositions.

Highly detuned optical fields in a Raman configuration have been used to coherently manipulate and create various superpositions of different atomic levels [20]. Similar optical manipulation techniques exist to couple BEC clouds in different internal states. Moreover, the OAM states of

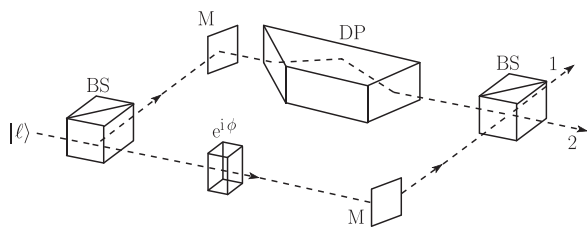


FIG. 1. Generation of superposition of the OAM states. The first beam splitter (BS) at the input is a $|\tilde{r}|^2/|\tilde{r}'|^2$ beam splitter as \tilde{r} and $i\tilde{r}'$ are the reflection and transmission amplitudes. The second beam splitter is 50:50, and the mirrors (M) are perfectly reflecting. The dove prism (DP) performs the operation $|\ell\rangle \rightarrow |-\ell\rangle$. Choosing $\phi = \pi$, and discarding the output at port 2, state $(\tilde{r}|\ell\rangle + \tilde{r}'|-\ell\rangle)$ is obtained at port 1.

light have also been shown to be useful for excitation of vortices in BEC through time-dependent linearly varying two-photon detuning [12] and through the STIRAP [21] type scheme [13]. In the following we discuss a Raman-type scheme to generate a superposition of vortex states in a BEC.

The level scheme for our model is depicted in Fig. 2. An initially nonrotating state $|0\rangle$ is coupled optically via two Raman-type configurations of the external fields, (Ω_+, Ω_c) and (Ω_-, Ω_c) , through internal states $|i\rangle$ and $|i'\rangle$. The polarizations of the optical fields are taken as shown in the figure; thus the internal quantum numbers of the final states $|+\rangle$ and $|-\rangle$ are the same. The Rabi frequencies Ω_+ and Ω_- arise from the coupling of the BEC cloud with the two counterrotating components of the special optical vortex state generated through the configuration discussed in Fig. 1.

Noting that the optical fields are highly detuned, the intermediate states ($|i\rangle$ and $|i'\rangle$) are sparsely populated. Thus, they can be adiabatically eliminated from the equations. Within this adiabatic approximation we can write a modified set of Ginzburg-Pitaevskii-Gross (GPG) [22] equations for the multicomponent BEC trapped by the cigar-shaped trapping potential $\mathcal{V} = (m/2) \times (\omega_\perp^2 r^2 + \omega_z z^2)$, where ω_\perp and ω_z are the transverse and longitudinal trapping frequencies, respectively. Also m is the mass of the individual atoms in the BEC cloud. We note that $r = \sqrt{x^2 + y^2}$ is the transverse radial coordinate and ϕ is the azimuthal angle in the x - y plane that will be required later to describe the phase structure of the rotating BECs. The configuration-space representations of the states $|0\rangle$, $|+\rangle$ and $|-\rangle$, shown in Fig. 2, are taken to be Ψ_0 , Ψ_+ , and Ψ_- , respectively. Thus, including the Raman-type optical couplings arising from the adiabatic elimination of the intermediate state, we arrive at the modified GPG equations for the three relevant components of the BEC cloud

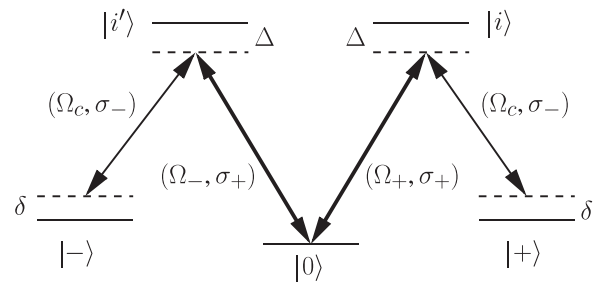


FIG. 2. The level scheme for generation of vortex state superposition. A nonrotating state $|0\rangle$ is coupled to the vortex states $|+\rangle$ and $|-\rangle$ through the optical vortex field components providing coupling strengths Ω_+ , Ω_- and a strong drive field with Rabi frequency Ω_c . The optical vortex beam is σ_+ polarized, whereas the drive field is σ_- polarized such that the hyperfine quantum number m_F is the same for the components $|0\rangle$, $|\pm\rangle$. The vorticity of the $|\pm\rangle$ states is $\pm\ell$, respectively.

$$i\hbar\dot{\Psi}_0 = \mathcal{H}\Psi_0 + \frac{\hbar}{\Delta} \left(\sum_{i=\pm} |\Omega_i|^2 \Psi_0 + \sum_{i=\pm} \Omega_i^* \Omega_c e^{-i\Delta t} \Psi_i \right)$$

$$i\hbar\dot{\Psi}_{\pm} = \mathcal{H}\Psi_{\pm} + \frac{\hbar}{\Delta} (|\Omega_c|^2 \Psi_{\pm} + \Omega_{\pm} \Omega_c^* e^{i\Delta t} \Psi_0), \quad (4)$$

where $\mathcal{H} = \mathcal{T} + \mathcal{V} - \mu + \eta(|\Psi_0|^2 + |\Psi_+|^2 + |\Psi_-|^2)$ is the self-energy operator which includes the kinetic (\mathcal{T}), potential (\mathcal{V}), and the interaction energy operators for the BEC states. Here $\eta = 4\pi\hbar a_{sc} N/m$ is the strength of the interparticle interactions of the N -particle BEC cloud, governed by the scattering cross section a_{sc} . Using the LG beam mode function Eq. (1), the Rabi frequencies corresponding to the coupling between the optical vortex beam superposition $a_+|\ell\rangle + a_-|-\ell\rangle$ and the BEC cloud can be written as

$$\Omega_{\pm}(\mathbf{r}) = a_{\pm} \Omega_0 e^{-r^2/w^2} (\sqrt{2}r/w)^{|\ell|} e^{\pm i\ell\phi} e^{ikz}, \quad (5)$$

where Ω_0 is the usual atom-field interaction Rabi frequency. The amplitudes a_{\pm} are respectively \tilde{t} and \tilde{r} corresponding to the first beam-splitter transmission and reflection amplitudes of the configuration shown in Fig. 1. With the size of the condensate chosen to be much smaller than the Laguerre-Gaussian beam waist, the exponential dependence on the radial coordinate in Eq. (5) can be ignored. Now we make an ansatz that the topological structure of the states $|0\rangle, |\pm\rangle$ are given by

$$\Psi_0(\mathbf{r}, t) = \alpha(t) \exp[i(\mu/\hbar - \kappa)t] \psi_g(\mathbf{r}), \quad (6a)$$

$$\Psi_{\pm}(\mathbf{r}, t) = \beta_{\pm}(t) \exp[i(\delta + \mu/\hbar - \kappa)t] \psi_{v\pm}(\mathbf{r}),$$

where the nonrotating component $\psi_g(\mathbf{r})$ and the rotating vortex components $\psi_{v\pm}(\mathbf{r})$ are given by

$$\psi_g(\mathbf{r}) = \exp\{-(1/2)[(r/L_{\perp})^2 + (z/L_z)^2]\} / \pi^{3/4} L_{\perp} L_z^{1/2}$$

$$\psi_{v\pm}(\mathbf{r}) = (x \pm iy)^{|\ell|} / \sqrt{|\ell|!} L_{\perp}^{|\ell|} \psi_g(\mathbf{r}). \quad (6b)$$

Here L_{\perp} and L_z are the size parameters of the condensate in the x - y plane and the z directions, respectively, and δ is the two-photon detuning as shown in Fig. 2. Thus, the time dependence of the populations of different components ($|\alpha(t)|^2, |\beta_{\pm}(t)|^2$) can be studied by projecting the rate Eqs. (4) on to the topological states (6a). So far the equations are very general and no restriction exists on the OAM quantum number ℓ . Hereafter, for convenience, we resort to a particular value of $\ell = 2$. However, one may note that the general idea would remain valid for any given ℓ . Thus, taking the projections onto the specified rotating or nonrotating states we arrive at

$$i\dot{\alpha}(t) = 3\kappa|\alpha(t)|^2\alpha(t) + \omega_{\perp}[a_+^*\beta_+(t) + a_-^*\beta_-(t)]$$

$$i\dot{\beta}_{\pm}(t) = \left[\delta + 2\omega_{\perp} + \frac{\kappa}{2} \sum_{i=\pm} |\beta_i(t)|^2 \right] \beta_{\pm}(t) + \omega_{\perp} a_{\pm} \alpha(t). \quad (7)$$

Here, the interparticle interaction strength appears through the parameter $\kappa = \pi\hbar a_{sc} N / [m(2\pi)^{3/2} L_{\perp}^2 L_z]$. This set of

equations can be solved numerically, using the experimental parameters for a ^{87}Rb BEC [23] (i.e., $\omega_{\perp} = 132$ Hz, $a_{sc} = 5$ nm, $L_{\perp} = 2.35$ μm , $L_z = 1.4$ μm), so that $\kappa = 422$ Hz. The results of our numerical studies are summarized in Fig. 3. We define a transfer function $f(t) = |\alpha(t)|^2 - |\beta_+(t)|^2 - |\beta_-(t)|^2$, which signifies the amount of population transferred from state $|0\rangle$ to states $|\pm\rangle$. Initially $f(t=0) = 1$ as all the population resides in the nonrotating ground state. If complete transfer is achieved to an appropriate superposition of the $|\pm\rangle$ states then $f(t) \rightarrow -1$. The transfer function, $f(t)$, is plotted for various values of the two-photon detuning δ in Fig. 3(a). The result is that only a continuous time variation of the detuning, achievable by changing the frequency of the second optical field, leads to complete population transfer at the steady state. Since the interaction terms in Eq. (7) effectively lead to time-dependent energy shifts of the vortex states as they begin to get occupied, only a time varying detuning maintains effective two-photon resonance to give complete population transfer. Furthermore, the BEC vortex state at the steady state can be shown to be $a_+^*|+\rangle + a_-^*|-\rangle$ when the input optical vortex state is $a_+|\ell\rangle + a_-|-\ell\rangle$, i.e., the phase difference between the BEC vortex components is negative of that between the optical vortex components. Figures 3(b)–3(d) show generation of various superpositions of the vortex states $|\pm\rangle$ for the time varying detuning.

The resulting vortex-superposition state could be detected by imaging its particle density distribution, which is proportional to an interference pattern of its components. Figure 4 shows x - y cross section of this interference pattern for a particular vortex state $\alpha|\ell = +3\rangle + \beta e^{i\phi}|-\ell = -3\rangle$. The pattern contains $m = 2\ell$ lobes and the visibility

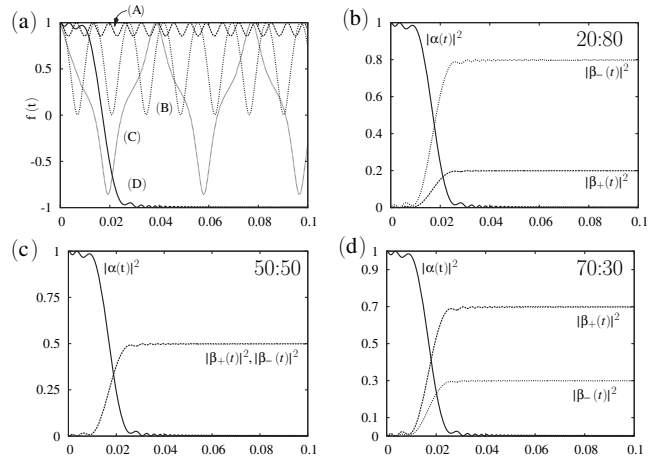


FIG. 3. (a) Transfer function $f(t)$ for various detunings. (A) $\delta = 0$, (B) $\delta = 900$, (C) $\delta = 380$, (D) linearly varying detuning $\delta(t) = 3000 - 400t$. All detunings are given in Hertz. The complete population transfer to the vortex state, corresponding to $f(t) = -1$ for sufficiently large t (measured in seconds), is possible only with time-dependent detuning. (b)–(d) show various superpositions of the vortex states. The steady state ratios are given in the notation $|\beta_+|^2 : |\beta_-|^2$.

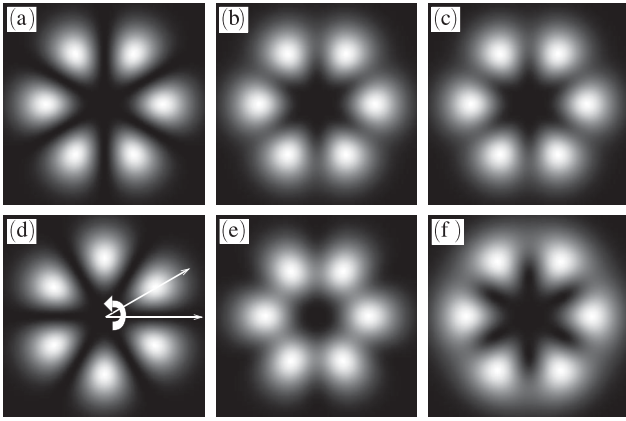


FIG. 4. Detection of the vortex superposition through characteristic interference of a general normalized state $\alpha|+\ell\rangle + \beta e^{i\phi}|-\ell\rangle$. $\ell = 3$ and $\phi = 0$ unless specified otherwise. (a) $\alpha^2:\beta^2 = 1:1$; $V = 1$, giving $m = 2\ell$ lobes in the interference pattern. (b) $\alpha^2:\beta^2 = 0.1:0.9$; $V = 0.6$. (c) $\alpha^2:\beta^2 = 0.9:0.1$; $V = 0.6$. Patterns (b) and (c) are identical. (d) Phase determination: $\alpha^2:\beta^2 = 1:1$, $\phi = \pi$; $V = 1$, notice rotation of the pattern with respect to that of (a) by an angle ϕ/m . After adding one more unit of OAM in the superposition to arrive at $\alpha|+\ell+1\rangle + \beta e^{i\phi}|-\ell+1\rangle$ distinct patterns (e) and (f) are obtained instead of (b) and (c).

$V = 2\alpha\beta$ gives the measure of the asymmetry in the amplitudes. The pair $\{\alpha, \beta\}$ can be determined using measured V and the normalization condition $\alpha^2 + \beta^2 = 1$. However, this does not assign the amplitudes to the states $|+\rangle$ or $|-\rangle$ with certainty, as the patterns in Figs. 4(b) and 4(c) are identical. We propose shining a OAM $= +1$ light of σ_+ polarization to obtain the vortex state $\alpha|3+1\rangle + \beta e^{i\phi}|-3+1\rangle$, the resulting interference pattern is shown in Figs. 4(e) and 4(f), which clearly differentiates between the two amplitude values giving rise to same visibility in Figs. 4(b) and 4(c). The phase difference ϕ causes rotation of the whole pattern by an amount ϕ/m as shown in Fig. 4(d). Existing theoretical schemes for detecting vortex states [24] could also be extended to detect a superposition of vortex states.

To conclude, we have devised a scheme to generate superposition of two counterrotating optical vortices. We have designed a Raman-type scheme to transfer the optical vortex superposition onto a superposition of vortices in BEC. We have suggested a detection scheme based on observing the particle density distribution. The macroscopic superpositions of vortices could have important fundamental as well as practical applications.

Part of this work was carried out (by K. T. K.) at the Jet Propulsion Laboratory under a contract with the National Aeronautics and Space Administration (NASA). K. T. K. acknowledges support from the National Research Council and NASA, Codes Y and S. Also K. T. K. wishes to thank Professor K.-P. Marzlin for useful discussions. K. T. K. and J. P. D. wish to thank Professor M. S. Zubairy for useful

discussions. J. P. D. acknowledges support from the Horace C. Hearne, Jr. Foundation, the Advanced Research and Development Activity, the Army Research Office, the National Security Agency, and the National Reconnaissance Office.

*Electronic address: Kishor.T.Kapale@jpl.nasa.gov

- [1] M. A. Nielsen and I. L. Chuang, *Quantum Computation and Quantum Information* (Cambridge University Press, Cambridge, England, 2000).
- [2] M. H. Anderson *et al.*, *Science*, **269**, 198 (1995); C. C. Bradley, C. A. Sackett, J. J. Tollett, and R. G. Hulet, *Phys. Rev. Lett.* **75**, 1687 (1995); M.-O. Mewes *et al.*, *Phys. Rev. Lett.* **77**, 416 (1996).
- [3] J. R. Abo-Shaeer, C. Raman, J. M. Vogels, and W. Ketterle, *Science* **292**, 476 (2001).
- [4] N. R. Heckenberg, R. McDuff, C. P. Smith, and A. G. White, *Opt. Lett.* **17**, 221 (1992); G. S. Agarwal, R. R. Puri, and R. P. Singh, *Phys. Rev. A* **56**, 4207 (1997).
- [5] J. Arlt, K. Dholakia, L. Allen, and M. J. Padgett, *J. Mod. Opt.* **45**, 1231 (1998).
- [6] K. Sueda, G. Miyaji, N. Miyanaga, and N. Nakatsuka, *Opt. Express* **12**, 3548 (2004).
- [7] D. Akamatsu and M. Kozuma, *Phys. Rev. A* **67**, 023803 (2003).
- [8] G. Molina-Terriza, J. P. Torres, and L. Torner, *Phys. Rev. Lett.* **88**, 013601 (2002); M. S. Bigelow, P. Zerom, and R. W. Boyd, *Phys. Rev. Lett.* **92**, 083902 (2004).
- [9] J. Leach *et al.*, *Phys. Rev. Lett.* **88**, 257901 (2002).
- [10] D. G. Grier, *Nature (London)* **424**, 810 (2003).
- [11] A. Mair, A. Vaziri, G. Weihs, and A. Zeilinger, *Nature (London)* **412**, 313 (2001).
- [12] K.-P. Marzlin, W. Zhang, and E. M. Wright, *Phys. Rev. Lett.* **79**, 4728 (1997).
- [13] G. Nandi, R. Walser, and W. P. Schleich, *Phys. Rev. A* **69**, 063606 (2004).
- [14] Z. Dutton and J. Ruostekoski, *Phys. Rev. Lett.* **93**, 193602 (2004).
- [15] Y. Nakamura, Yu. A. Pashkin, and J. S. Tsai, *Nature (London)* **398**, 786 (1999); J. R. Friedman *et al.*, *Nature (London)* **406**, 43 (2000); C. H. van der Wal *et al.*, *Science* **290**, 773 (2000).
- [16] A. Vaziri, G. Weihs, and A. Zeilinger, *J. Opt. B* **4**, S47 (2002).
- [17] L. Allen, M. W. Beijersbergen, R. J. C. Spreeuw, and J. P. Woerdman, *Phys. Rev. A* **45**, 8185 (1992).
- [18] M. J. Padgett and J. P. Lesso, *J. Mod. Opt.* **46**, 175 (1999).
- [19] A. Zeilinger, *Am. J. Phys.* **49**, 882 (1981).
- [20] Y. Niu, S. Gong, R. Li, and S. Jin, *Phys. Rev. A* **70**, 023805 (2004).
- [21] K. Bergmann, H. Theuer, and B. W. Shore, *Rev. Mod. Phys.* **70**, 1003 (1998).
- [22] M. Edwards *et al.*, *Phys. Rev. A* **53**, R1950 (1996).
- [23] D. S. Jin *et al.*, *Phys. Rev. Lett.* **77**, 420 (1996).
- [24] E. L. Bolda and D. F. Walls, *Phys. Rev. Lett.* **81**, 5477 (1998); E. V. Goldstein, E. M. Wright, and P. Meystre, *Phys. Rev. A* **58**, 576 (1998).